SOLVING MULTI CONSTRAINTS STRUCTURAL TOPOLOGY OPTIMIZATION PROBLEM WITH REFORMULATION OF LEVEL SET METHOD

I. Manafi[1] and S. Shojaee[2*, †]
[1]*Department of Civil Engineering, Graduate University of Technology, Kerman, Iran*
[2]*Department of Civil Engineering, Shahid Bahonar University, Kerman, Iran*

ABSTRACT

Due to the favorable performance of structural topology optimization to create a proper understanding in the early stages of design, this issue is taken into consideration from the standpoint of research or industrial application in recent decades. Over the last three decades, several methods have been proposed for topology optimization. One of the methods that has been effectively used in structural topology optimization is level set method. Since in the level set method, the boundary of design domain is displayed implicitly, this method can easily modify the shape and topology of structure. Topological design with multiple constraints is of great importance in practical engineering design problems. Most recent topology optimization methods have used only the volume constraint; so in this paper, in addition to current volume constraint, the level set method combines with other constraints such as displacement and frequency. To demonstrate the effectiveness of the proposed level set approach, several examples are presented.

1. INTRODUCTION

Nowadays structural topology optimization problems are very significant and demanding in many engineering fields and they are capable of speeding up the structural design process and producing valid and reliable solutions to different engineering problems. This branch of engineering science has made considerable progress in last three decades So far, considerable researches and several topology optimization methods such as homogenization

---
*Corresponding author: Department of civil engineering, Shahid Bahonar University, Kerman, Iran
†E-mail address: saeed.shojaee@uk.ac.ir (S. Shojaee)

methods (Bendsøe and Kikuchi [1]; Suzuki and Kikuchi [2]; Allaire and Kohn [3]; Allaire et al. [4]), Solid Isotropic Material with Penalization (SIMP) methods (Bendsøe [5]; Bendsøe and Sigmund 2003 [6]); Evolutionary Structural Optimization (ESO) methods (Xie and Steven [7]) and topology optimization based ant colony methodology (Kaveh et. al. [8]) have been suggested. The initial research on Bi-directional evolutionary Structural optimization (BESO) was carried out by Yang et al. [9] for stiffness optimization. The BESO notion has also been applied to 'full stress design' by using the von Mises stress criterion (Querin et al. [10]). A new BESO algorithm for stiffness optimization developed by authors (Huang and Xie [11]) which addresses many issues related to topology optimization of continuum structures such as a proper statement of the optimization problem, checkerboard pattern, mesh-dependency and convergence of solution. Recently, the level set methods (Osher and Sethian [12]), which were initially proposed for following the propagation of fluid interfaces, have been applied into structural topology optimization effectively [13], [14]. In this method the boundaries of design domain are implicitly described by the zero level set of a higher dimensional function. Therefore, level set method (LSM) can easily control various shape and topology changes such as combining, separating and developing sharp corners. A binary and piecewise constant level set method have been applied into structural topology optimization [15], [16], which increases the convergence speed.

One limitation of the proposed methods is to use the volume constraint alone. So, in this paper, the level set approach for topology optimization of continuum structures is presented with constraints of displacement and frequency in addition to the current volume constraint. The displacement constraint reflects certain functional requirements that the deformation at some points needs to be under admissible bound. The frequency constraint comes from the design need for a structure to prevent large deformation caused by amplification effects due to external incitements such as wind or earthquake etc. In order to show the efficiency of the suggested level set method, various examples are presented.

The subsequent sections are organized as follows. The second section introduces the standard level set method. The third section describes the numerical implementation of applying the algorithms to compliance minimization with volume, displacement and frequency constraints and concludes the search algorithms for the Lagrange multipliers. The fourth section represents a series of numerical examples of the selected optimization problem. The conclusions are drawn in the last section.

2. LEVEL SET METHOD

The level set approach, first presented in [12], has become a powerful tool for calculating and analyzing the movement of an interface in two or three dimensions. It has been used in many fields, such as image processing, solids modeling, fluid mechanics, and combustion. The basic concept of level set methods is defined here to provide essential background for later parts.

2.1 Implicit interface representations

In the level set framework, an interface Γ (curve or surface) is shown implicitly through a

level set function $\phi(x)$ and the interface itself is the zero level set. Mathematically, it can be defined as:

$$\Gamma = \left\{ x;\ \phi(x) = 0, x \in D \right\} \tag{1}$$

where D is a domain which includes Γ entirely. To describe a structure Ω, we represent the following definition:

$$\begin{cases} \phi(x) < 0 : & \forall\ x \in D \backslash \Omega \\ \phi(x) = 0 : & \forall\ x \in \partial\Omega \\ \phi(x) > 0 : & \forall\ x \in \Omega \backslash \partial\Omega \end{cases} \tag{2}$$

where $\Omega \subset D$ is a fixed domain which contains all acceptable figures of $\Omega = \left\{ x \mid x \in D, \phi(x) \geq 0 \right\}$. $\phi(x) < 0$ and $\phi(x) > 0$ show interior and exterior of design domain respectively and $\phi(x) = 0$ shows the function value on the design domain.

2.2 Level set equation

Level set methods add dynamics to implicit interfaces. The implicit representation of design domain boundary is very flexible and has the capability of merging and splitting boundaries. In the other words, with modifying $\phi(x)$, the zero level of this function is changed either. The implicit function $\phi(x)$ is used both to represent the interface and to evolve the interface. In the entire evolutionary process of level set function, the value of this function is equal to zero on design domain boundary. If we take derivative of the following equation with respect to t:

$$\phi(x) = 0.0 \qquad , \forall x \in \partial\Omega \tag{3}$$

We get an advection equation from the chain rule:

$$\frac{\partial \phi}{\partial t} + \nabla \phi . v(x) = 0.0 \tag{4}$$

where $v(x) = \dfrac{dx}{dt}$ is the velocity vector field. Since $n = \dfrac{\nabla \phi}{\left| \nabla \phi \right|}$ and $v.\nabla \phi = (v_n)\left| \nabla \phi \right|$, we can replace equation (4) with below equation:

$$\frac{\partial \phi}{\partial t} + v_n \left| \nabla \phi \right| = 0.0 \tag{5}$$

where v_n is the normal velocity vector. Equations (4) and (5) are called level set equations.

This partial differential equation describes the motion of the interface where $\phi(x) > 0$ under the velocity v_n. The main advantage of implicit demonstration is the capability to handle topological changes, such as separating and merging of the boundary in a natural way.

It should be noted that in some literature, the description of interior and exterior of the design domain in equation. (2) is reversed:

$$\begin{cases} \phi(x) > 0 : & \forall\ x \in D \setminus \Omega \\ \phi(x) = 0 : & \forall\ x \in \partial\Omega \\ \phi(x) < 0 : & \forall\ x \in \Omega \setminus \partial\Omega \end{cases} \tag{6}$$

So in this case the normal n changes to:

$$n = -\frac{\nabla\phi}{|\nabla\phi|} \tag{7}$$

And the level set equation becomes:

$$\frac{\partial\phi}{\partial t} - v_n |\nabla\phi| = 0.0 \tag{8}$$

3. LEVEL SET METHOD FOR TOPOLOGY OPTIMIZATION OF MULTI-CONSTRAINED PROBLEMS

We want to employ the level set method for solving structural topology optimization problems with multiple constraints. The optimization problem is to minimize the compliance of a solid structure subject to volume, displacement and frequency constraint. The following is the mathematical definition of the problem:

$$Minimize\ \ C = C(X) = u^T K u = \sum_{i=1}^{N} u_i^T k_i^p u_i = \sum_{i=1}^{N} x_i u_i^T k_1^p u_i \tag{9}$$

$$subject\ to : \begin{cases} V(X) = V_{req} \\ d_j(X) - d^* < 0 \\ \omega^* - \omega_n(X) < 0 \end{cases} \tag{10}$$

$$Ku = F \tag{11}$$

$$x_i = 0\ \ or\ \ x_{min}\ \ \ \ \forall\ i = 1,...,N \tag{12}$$

where $X = \{x_1, ..., x_N\}$ is the vector of element "densities", with entries of $x_i = x_{\min}$ for a void element and $x_i = 1$ for a solid element, where i is the element index, $C(X)$ is the compliance objective function, u is the displacement vector, K is the global stiffness matrix, p is the penalty exponent, d_j is the displacement magnitude of the jth node, ω_n is the nth natural frequency, with d^* and ω^* being the imposed constraint values. The displacement and the frequency constraints are demonstrated in equation (10). In some cases, the natural frequencies may need to be bounded under a certain limit in order to avoid from the hazardous frequency range. In such scenarios, the frequency constraint is varies to $\omega_n(x) - \omega^* > 0$ and the later Lagrange function changes accordingly. The binary design variable nature is defined in equation (12) where 1 is the upper limit of the design variable and $x_{\min}$ the lower limit. The design variable x_i indicates the corresponding element's status, namely presence (solid) or absence (void). In this formulation, elements are not really omitted from the structure by "removal" but substituted with very weak material. In this case, the design variable represents the element relative density with two candidate values: 1 indicating element presence, and $x_{\min}$ which is a very small quantity (i.e., 10^{-3}) demonstrating element absence. The volume constraint is defined in equation (10) with V_{req} the required volume fraction of final design volume.

The level-set method (Allaire et al. [13]; Wang et al. [14]) is applied to find a local minimum for the optimization problem. The method derives its name from the use of a level-set function for illustrating the structure. If the structure occupies some domain Ω the level-set function has the following definition:

$$\begin{cases} \phi(\text{s}) < 0 : & if \ s \in \Omega \\ \phi(s) = 0 : & if \ s \in \partial\Omega \\ \phi(s) > 0 : & if \ s \notin \Omega \end{cases} \tag{13}$$

where s is any point in the design domain, and $\partial\Omega$ is the boundary of.Ω. The following evolution equation is applied to update the level-set function and therefore the structure:

$$\frac{\partial\phi}{\partial t} + v_n |\nabla\phi| + \omega g = 0.0 \tag{14}$$

where t represents time, $v(s)$ and $g(s)$ are scalar fields over the design domain, and ω is a positive parameter which determines the effect of the term containing g. The field v determines geometric movement of structure boundary and is selected according to the shape derivative of the objective function. The term including g is a forcing term which determines the nucleation of new holes in the structure and is chosen based on the topological derivative of objective function.

If the parameter ω is zero, equation (14) is the standard Hamilton-Jacobi evolution

equation for a level-set function ϕ under a normal velocity of the boundary $v(s)$, taking the boundary normal in the outward direction from Ω (e.g., Osher and Fedkiw [12]). The simpler equation without the term involving g is typically used in level-set methods for topology optimization (e.g., Allaire et al. [13]; Wang et al. [14]). However, on two dimensional problems, this standard evolution equation has the main difficulty that new void areas can not be nucleated in the structure (Allaire et al. [13]). Here, the supplementary forcing term including g is added following Burger et al. ([17]) to verify that new holes can nucleate within the structure during the optimization procedure.

To form a topology optimization algorithm, the level-set function can be discretized with gridpoints centered on the elements of the mesh. If p_i shows the center position of element i, then the discretized level-set function ϕ satisfies:

$$\Gamma = \{x; \ \phi(x) = 0, x \in D\} \tag{15}$$

Then, the discretized level-set function ϕ can be updated to locate a new structure by solving equation (14) in a numerical manner. ϕ is initialized as a signed distance function and an upwind finite difference scheme is applied so that the evolution equation can be solved precisely. Furthermore, the time step for the finite difference scheme is chosen to satisfy the CFL stability condition:

$$\Delta t \leq \frac{h}{\max|v|} \tag{16}$$

where h is the minimum distance between neighbor gridpoints within the spatial discretization and the maximum is chosen over all gridpoints (e.g., Osher and Fedkiw [12]).

As stated above, the two scalar fields v and g are typically selected according to shape and topological sensitivities of the objective function, respectively. In order to satisfy the volume constraint, here they are chosen using the shape and topological sensitivities of the Lagrangian

$$L = C(x) + \lambda^K \left[V(x) - V_{req} \right] + \frac{1}{2\Lambda^K} \left[V(x) - V_{req} \right]^2 \tag{17}$$

where λ^K and Λ^K are parameters which vary with each iteration K of the optimization algorithm. They are updated applying the below approach:

$$\lambda^{K+1} = \lambda^K + \frac{1}{\Lambda^K} \left[V(x) - V_{req} \right] \tag{18}$$

$$\Lambda^{K+1} = \alpha \Lambda^K \tag{19}$$

where $\alpha \in (0,1)$ is a constant parameter. This implements the augmented Lagrangian

multiplier approach for constrained optimization, as applied for topology optimization with the level-set approach by Luo et al. [18].

The normal velocity v is chosen as a descent direction for the Lagrangian L applying its shape derivative (e.g., Allaire et al. [13]; Wang et al. [14]). In the case of traction-free boundary conditions on the moving boundary, the shape sensitivity of the compliance objective $C(X)$ is the negative of the strain energy density: (e.g., Allaire et al. [13]):

$$\frac{\partial C}{\partial \Omega}\big|_i = -u_i^T k_i^p u_i \tag{20}$$

The shape sensitivity of the volume $V(X)$ is

$$\frac{\partial V}{\partial \Omega}\big|_i = 1 \tag{21}$$

Using these shape sensitivities, the normal velocity v within element i at iteration k of the algorithm is

$$v\big|_i = -\frac{\partial L}{\partial \Omega} = u_i^T k_i^p u_i - \lambda^K - \frac{1}{\Lambda^K}\left[V(x) - V_{req}\right] \tag{22}$$

According to Burger et al. [17], the forcing term g should be taken as

$$g = -sign(\phi)D_T L \tag{23}$$

where $D_T L$ is the topological sensitivity of the Lagrangian L. For compliance minimization, nucleating solid areas in the void regions of the design is meaningless because such solid areas will not take any load. Hence, holes should only be nucleated in the solid structure.

$$g = \begin{cases} D_T L & if \ \phi < 0 \\ 0 & if \ \phi \geq 0 \end{cases} \tag{24}$$

The topological sensitivity of the compliance objective function in two dimensions with traction-free boundary conditions on the nucleated hole with the unit ball as the model hole is (e.g., Allaire et al. [23]).

$$D_T C = \frac{\pi(\lambda + 2\mu)}{2\mu(\lambda + \mu)}\left\{4\mu u_i^T k_i u + (\lambda - \mu)u_i^T (k_{tr})_i u\right\} \tag{25}$$

where $u_i^T (k_{tr})_i u$ is the finite element approximation to the product $tr(\sigma)tr(\varepsilon)$ where σ is the stress tensor and ε is the strain tensor. In (23), λ and μ are the Lamé constants for the

solid material. The topological sensitivity of the volume $V(\mathbf{x})$ when the model hole is the unit ball is

$$D_T V(x) = -\pi \tag{26}$$

Putting these results into the description of the Lagrangian and using (24) gives the source term g.

$$g = D_T L = \frac{\pi(\lambda + 2\mu)}{2\mu(\lambda + \mu)} \left\{ 4\mu u_i^T k_i u + (\lambda - \mu) u_i^T (k_{tr})_i u \right\} - \lambda\pi - \frac{\pi}{\Lambda} \left[V(x) - V_{req} \right] \tag{27}$$

3.1 Augmented Lagrangian function for topology optimization problems with volume, displacement and frequency constraints

In this section, objective function combines with volume, displacement and frequency constraints via augmented Lagrangian method:

$$\begin{aligned} L = C(x) + \lambda^K \left[V(x) - V_{req} \right] + \frac{1}{2\Lambda^K} \left[V(x) - V_{req} \right]^2 \\ + \theta(d_j - d^*) + \gamma(\omega^* - \omega_n) \end{aligned} \tag{28}$$

where θ and γ are Lagrangian multipliers.

3.1.1 Calculating Lagrangian function sensitivity

The sensitivity of optimization problem is calculated by forming Lagrangian function with constraints of volume, local displacement and natural frequency as follows.

If the volume term equal to parameter R :

$$R = \lambda^K \left[V(x) - V_{req} \right] + \frac{1}{2\Lambda^K} \left[V(x) - V_{req} \right]^2 \tag{29}$$

Then the sensitivity of the Lagrange function, calculated according to the following equation:

$$\alpha_i = \frac{\partial C}{\partial x_i} + \frac{\partial R}{\partial x_i} + \mu \frac{\partial d_j}{\partial x_i} - \gamma \frac{\partial \omega_n}{\partial x_i} = \alpha^{stf} + \alpha^{vol} + \theta\alpha^{dis} - \gamma\alpha^{frq} \tag{30}$$

It is seen that the element sensitivity number of the total Lagrange function is a combination of the element sensitivities of the mean compliance α^{stf}, volume α^{vol}, the local displacement on the jth node α^{dis}, and the nth natural frequency α^{frq}. So the overall sensitivity calculation is defined with these four terms.

3.1.2 Sensitivity calculation for displacement and frequency constraints

The element sensitivity for stiffness optimization is commonly calculated as the element strain energy density (such as in Bendsøe and Sigmund [6]). The calculation use SIMP material model (Bendsøe and Sigmund [24]) that describes the element Young's modulus through the following power law penalization.

$$E(x_i) = E^0 x_i^p \qquad (31)$$

where p is the penalty exponent and E^0 is the Young's modulus of solid material, i.e. when $x_i = 1$. According to this material model, the element sensitivity for the mean compliance defines as below (Huang and Xie [27]).

$$\alpha_i^{stf} = \frac{\partial C}{\partial x_i} = -\frac{px_i^{p-1}}{2} u_i^T K_i^0 u_i \qquad (32)$$

where u_i is the element displacement vector, K_i^0 is the element stiffness matrix calculated with solid material, i.e. using the Young's modulus E^0 . With the same material model, the element sensitivity for the displacement (Huang and Xie [28]) is defined as

$$\alpha_i^{dis} = \frac{\partial d_j}{\partial x_i} = px_i^{p-1} u_{ij}^T K_I^0 u_i \qquad (33)$$

where u_{ij} is the element displacement vector under the virtual load.

In order to prevent the artificial and localized modes, a modified SIMP material model (Huang *et al.* [29]) suggested as

$$E(\mathrm{x}_i) = \left[\frac{x_{\min} - x_{\min}^p}{1 - x_{\min}^p} (1 - x_i^p) + x_i^p \right] E^0 \qquad (34)$$

With the help of the above modified SIMP material model, the element sensitivity for the natural frequency is calculated as the following. More details of this material model and frequency sensitivity calculation are found in (Huang *et al.* [29]). Alternative material models can be also seen in (Pedersen [30]).

$$\alpha_i^{frq} = \frac{\partial \omega_n}{\partial x_i} = \frac{1}{2\omega_n} u_{i,n}^T \times \left(\frac{1 - x_{\min}}{1 - x_{\min}^p} px_i^{p-1} K_i^0 - \omega_n^2 M_i^0 \right) u_{i,n} \qquad (35)$$

where $u_{i,n}$ indicates the element eigenvector of the nth mode and M_i^0 is the element mass matrix with solid material. Sometimes the neighbor eigenmodes may become multiple by

having the identical frequencies. In this sense, BESO methods simply takes the average of the sensitivities from the pertinent modes to solve this problem (see Yang *et al.* [31] or section 2.2 of Zuo *et al.* [32]).

Therefore, the shape and topology sensitivity of Lagrangian function in combination with volume, displacement and frequency defined as below

$$
\begin{aligned}
D_T L &= \frac{\pi(\lambda + 2\mu)}{2\mu(\lambda + \mu)} \left\{ 4\mu Ae(u).e(u) + (\lambda - \mu)tr(Ae(u))tr(e(u)) \right\} \\
&+ \pi \times (\lambda^k - \frac{1}{\Lambda}(V(x) - V_{req})) \\
&+ \theta p x_i^{p-1} u_{ij}^T K_I^0 u_i \\
&- \gamma \frac{1}{2\omega_n} u_{i,n}^T \times \left(\frac{1 - x_{\min}}{1 - x_{\min}^p} p x_i^{p-1} K_i^0 - \omega_n^2 M_i^0 \right) u_{i,n}
\end{aligned}
\tag{36}
$$

$$
\begin{aligned}
D_S L &= -u_i^T k_i^p u_i - (\lambda^k - \frac{1}{\Lambda}(V(x) - V_{req})) \\
&+ \theta p x_i^{p-1} u_{ij}^T K_I^0 u_i \\
&- \gamma \frac{1}{2\omega_n} u_{i,n}^T \times \left(\frac{1 - x_{\min}}{1 - x_{\min}^p} p x_i^{p-1} K_i^0 - \omega_n^2 M_i^0 \right) u_{i,n}
\end{aligned}
\tag{37}
$$

where θ and γ are the Lagrangian multiplier of displacement and frequency constraint respectively.

3.1.3 Determination of lagrange multiplier

Lagrange multipliers are presented as additional variables of the Lagrange function. They need to be determined in order, so that a solution for the optimization problem is obtained.

θ and γ are defined through a scaling function of replacement factors ϕ_d and ϕ_ω which range in a narrow domain [0 , 1). (see Zou *et al.* [32]).

$$
\begin{aligned}
\theta_j &= \frac{\varphi_d}{1 - \varphi_d}, & \gamma_j &\in [0,1) \\
\gamma_j &= \frac{\varphi_\omega}{1 - \varphi_\omega}, & \varphi_k &\in [0,1)
\end{aligned}
\tag{38}
$$

In the above description, the Lagrange multipliers are represented in an entire range with the replacement factors φ_d and φ_ω, e.g. zero φ_d leads θ_j to zero and φ_d approaching 1 pushes θ_j to infinity. Increasing or decreasing the Lagrange multipliers can be achieved by increasing or decreasing the relevant replacement factors. This way, the determination of

Lagrange multipliers is realized by the searching for replacement factors within $[0, 1)$ with suitable increments in programming implementation.

3.1.4 Satisfaction of displacement and frequency constraint

The volume constraint and the solution convergence are examined for a decision whether to finish the optimization process at the end of each iterative step. Furthermore, for the present problem, the satisfaction of the additional constraints such as displacement and frequency is checked with the average through the last iterative steps.

$$
\begin{aligned}
(\frac{1}{N}\sum_{i=1}^{N} d_{j,q-i+1}) - d^* < 0 \\
\omega^* - (\frac{1}{N}\sum_{i=1}^{N} \omega_{n,q-i+1}) < 0
\end{aligned}
\tag{39}
$$

where q is the current iterative step, and in this paper N is chosen to be 10 so that the additional constraints are satisfied in the last ten designs. The iterative process for description of the update scheme of the Lagrange multipliers is summarized into the steps shown in the flowchart of Fig. 1. (see Zou *et al.* [32]).
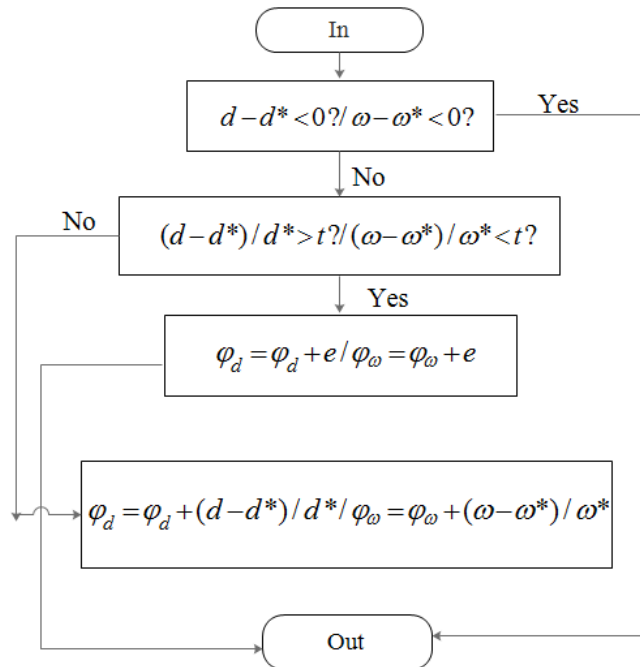
$$note: \text{the tolerance } t \text{ and increment } e$$
$$\text{can be prescribed as small numbers, e.g.1\%}$$

Figure 1. Flowchart of the lagrange multipliers determination

4. NUMERICAL EXAMPLES

Numerical examples are illustrated in this section using the suggested method described in final section. In this section, by examining several results in two dimensional problems, the validation of the suggested approach is affirmed. The finite element analysis is based on "ersatz material'' scheme [13], which fills the void areas with one weak material ($x_{min} = 10^{-2}$). All numerical examples have following data, Young's modulus is assumed $E = 1GPa$ and mass density is supposed $\rho = 8000 \frac{kg}{m^3}$, Poisson' ratio for materials is assumed 0.3. Lagrangian multiplier for volume is $\lambda = 0.01$, penalty multiplier is $\Lambda = 1000$ and penalty exponent is assumed $p = 3$.

4.1 Cantilever beam

Fig. 2 illustrates the design domain, loading and boundary condition of a cantilever beam. The boundary of the left side is fixed, and a beam is subject to vertical concentrated force F=100N at the middle of its right free side. The size of the design domain is 80×40 with a squared mesh size of 1×1 and the volume fraction is 30%.
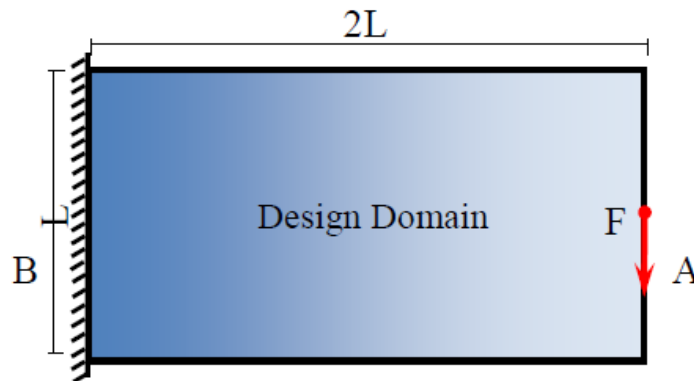

Figure 2. Design domain, loading and boundary condition of cantilever beam

Additional constraints on the vertical displacement d_A at point *A* and the fundamental frequency ω_1 are involved in the optimization of the cantilever beam. The additional constraints are combined into the following set: $\omega_1 > 1.9 \times 10^{-4}$ *rad / s* and $d_A < 10.5$ *mm*. The evolution procedure of the optimal topology is shown in Fig. 3 while the corresponding resulted performance is given in Table 1. Fig. 4 illustrates the evolutionary histories for the mean compliance, local displacement, fundamental frequency and volume fraction respectively. The convergence in the mean compliance satisfied during the last iterative steps for the optimization problem with multiple constraints.

Table 1: Summary of optimal design under volume, displacement and frequency constraints

Constraint	Compliance (Nmm)	Local displacement (mm)	Natural frequency (rad/s)
$\omega_1 > 1.9 \times 10^{-4}$ rad/s $d_A < 10.5$ mm	1094.14	10.49	1.917×10^{-4}

(a) Initial design   (b) Step 10   (c) Step 20

(d) Step 30   (e) Step 40   (f) Step 50

(g) Final design
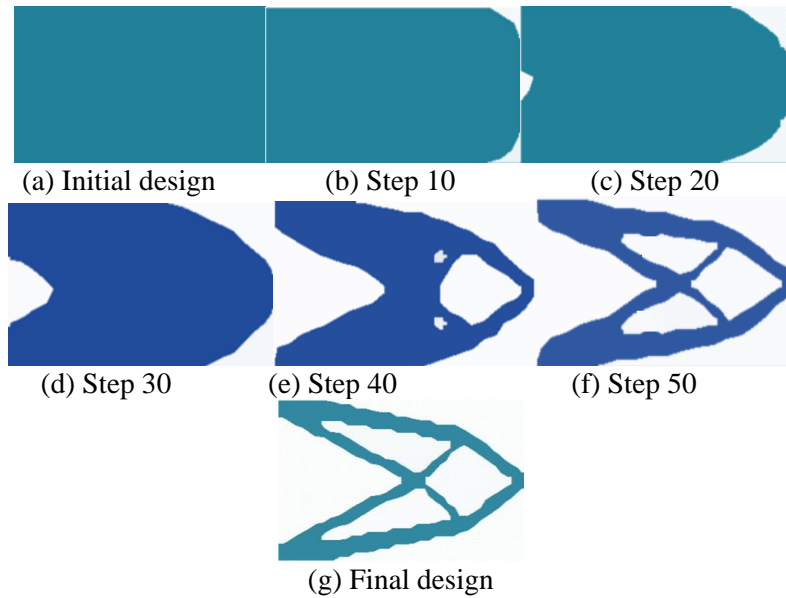
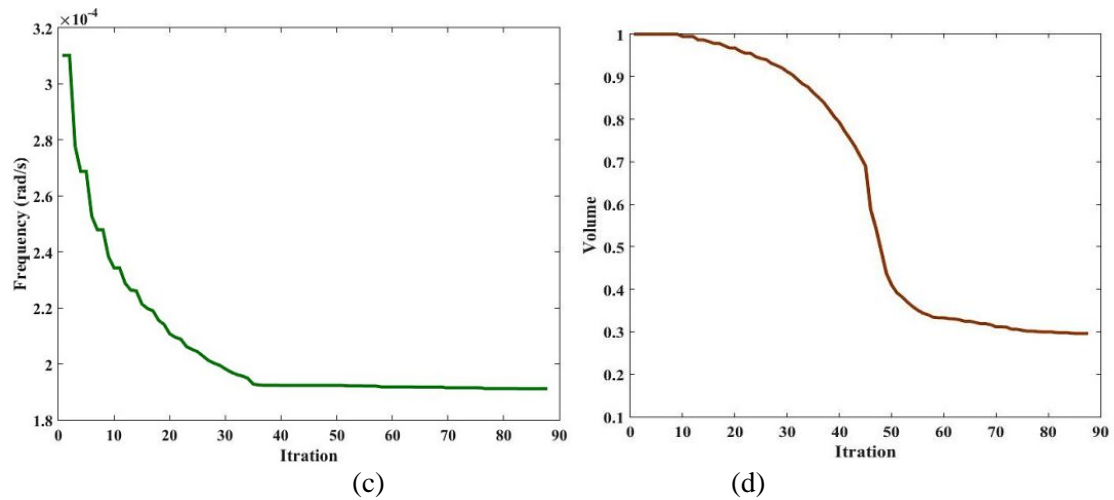Figure 3. The evolution process of optimal design for a cantilever beam

(a)

(b)

(c)   (d)
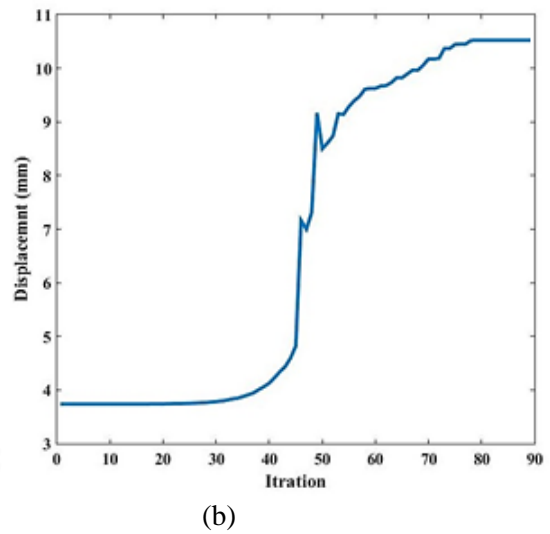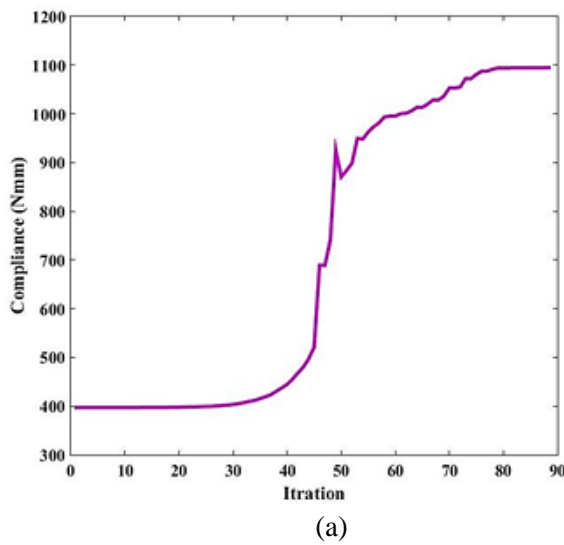
Figure 4. Evolutionary optimization histories for the optimal designs half wheel beam: (a) mean compliance; (b) local displacement; (c) fundamental frequency; (d) volume fraction

4.2 Half wheel beam

In the next example we consider a half wheel beam. The design domain, loading and boundary condition of this type of structure are shown in Fig. 5. The beam is simply supported at the lower corners and vertically loaded at the middle point of the upper edge. The roller-supported corner is denoted point *A* where a horizontal local displacement constraint is to be applied. The size of the design domain is 70×70 with a squared mesh size of 1×1 and the volume fraction is 30%.

Additional constraints on the horizontal displacement d_A at point *A* and the fundamental frequency ω_1 are involved in the optimization of the half wheel beam. The additional constraints are combined into the following set: $\omega_1 > 3.3 \times 10^{-3}$ *rad / s* and $d_A < 0.88$ *mm*.
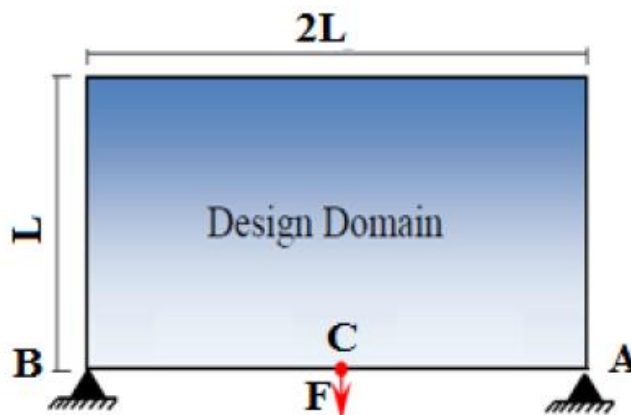

Figure 5. Design domain, loading and boundary condition of half wheel beam

(a) Initial design   (b) Step 10   (c) Step 20

(d) Step 30   (e) Step 45   (f) Step 50

(g) Final design

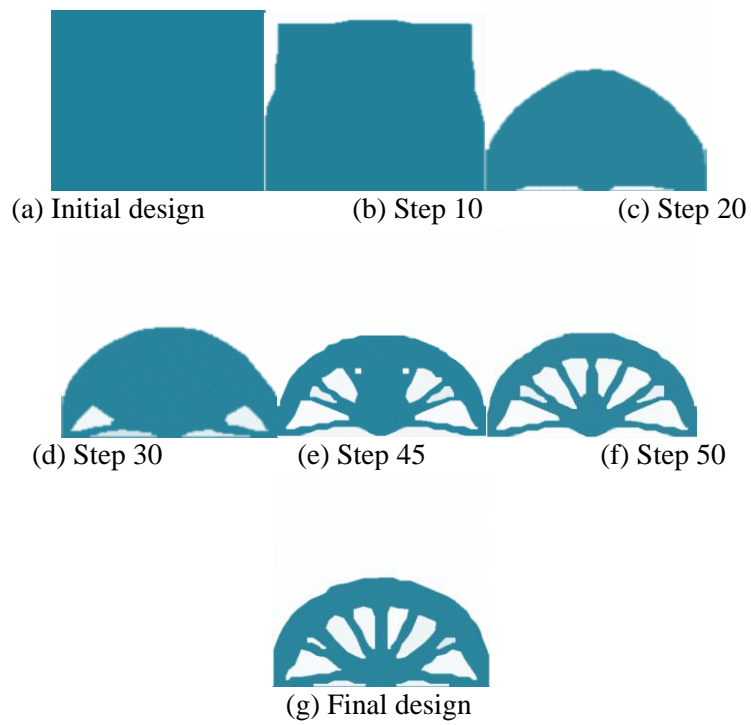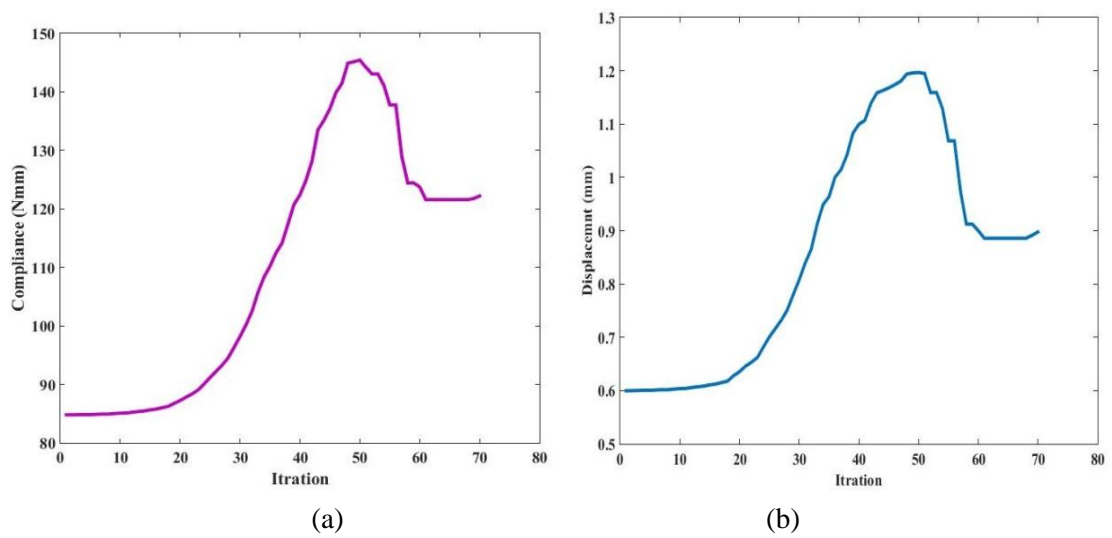Figure 6. The evolution process of optimal design for a cantilever beam

(a)   (b)

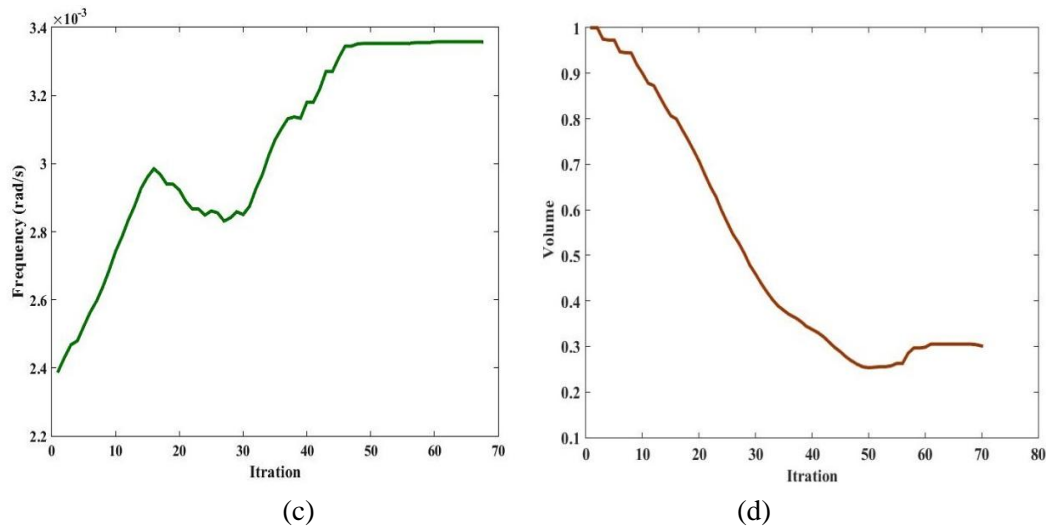(c)   (d)

Figure 7. Evolutionary optimization histories for the optimal designs half wheel beam: (a) mean compliance; (b) local displacement; (c) fundamental frequency; (d) volume fraction

Table 2: Summary of optimal design under volume, displacement and frequency constraints

Constraint	Compliance (Nmm)	Local displacement (mm)	Natural frequency (rad/s)
$\omega_1 > 3.3 \times 10^{-3}\ rad/s$ $d_A < 0.9\ mm$	122.23	0.8914	3.334×10^{-3}

4.3. Bridge type structure

As the final example, we want to consider the bridge type structure. The bridge is pinned at both lower corners and subject to a concentrated force $F = 100\ N$ at the center of the lower edge. The design domain, loading and boundary condition of this type of structure are shown in Fig. 8. The center of lower edge is denoted point C where a vertical local displacement constraint is to be applied. The size of the design domain is 80×40 with a squared mesh size of 1×1 and the volume fraction is 30%.

Additional constraints on the vertical displacement d_C at point C and the fundamental frequency ω_1 are included in the optimization of the bridge type structure. The additional constraints are combined into the following set: $\omega_1 > 1.6 \times 10^{-3}\ rad/s$ and $d_A < 1.5\ mm$.
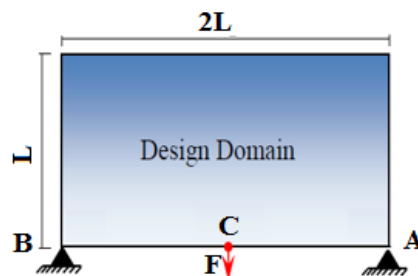

Figure 8. design domain, loading and boundary condition of bridge type structure

(a) Initial design   (b) Step 10   (c) Step 25

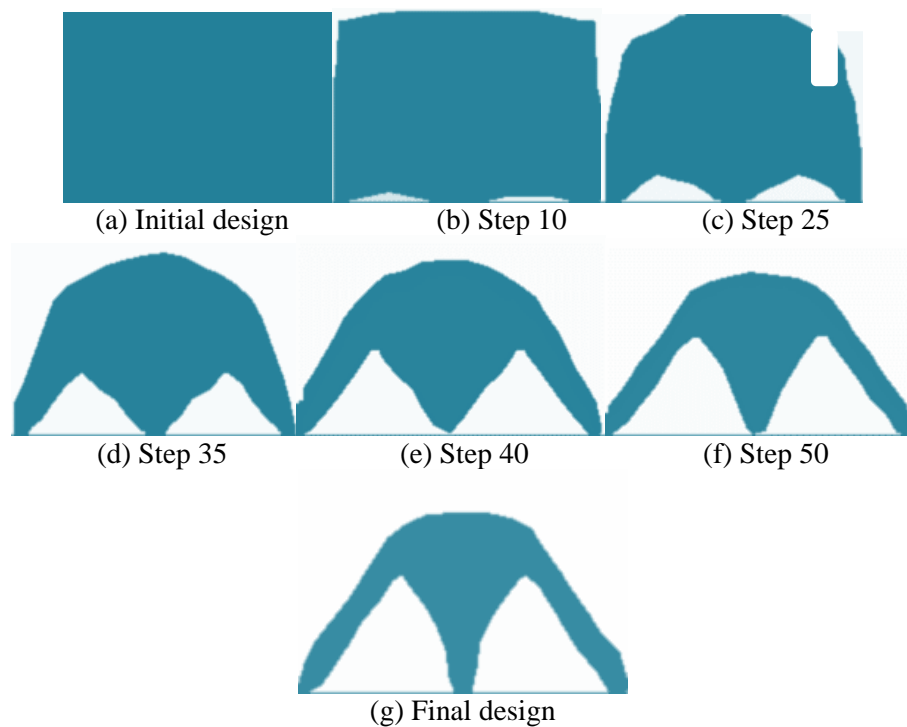(d) Step 35   (e) Step 40   (f) Step 50

(g) Final design

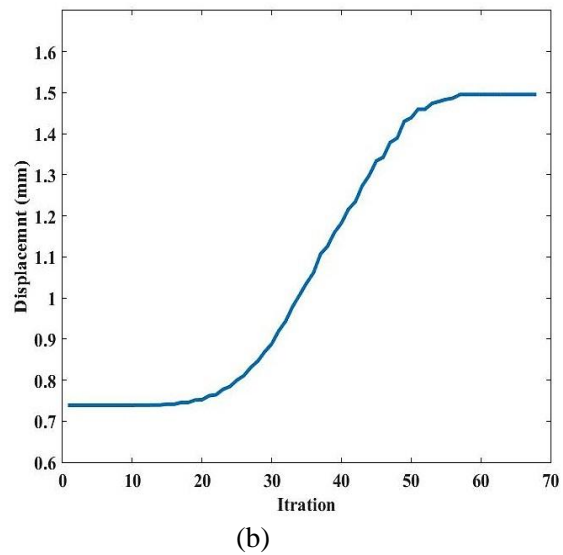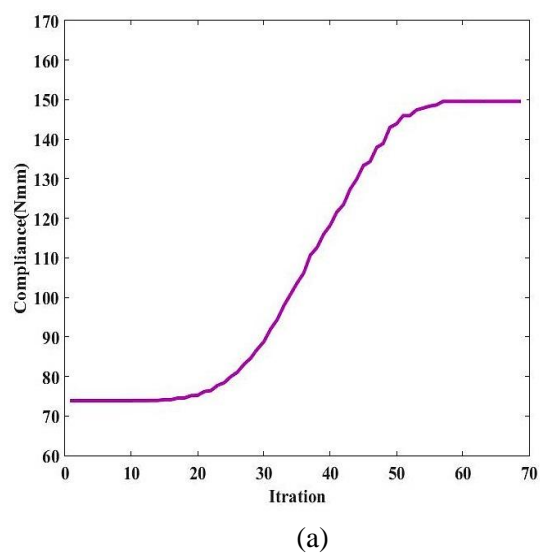Figure 9. The evolution process of optimal design for a cantilever beam

(a)

(b)

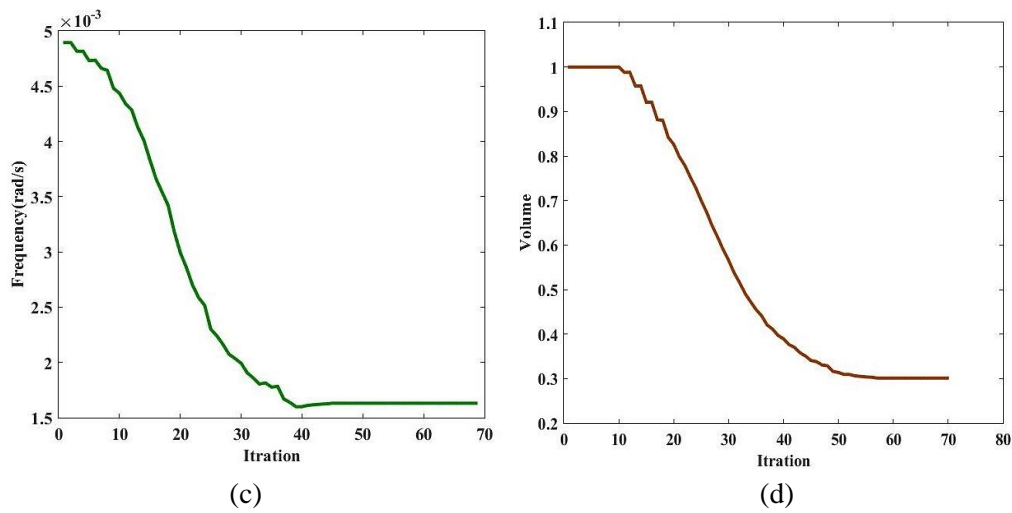(c)   (d)

Figure 10. Evolutionary optimization histories for the optimal designs half wheel beam: (a) mean compliance; (b) local displacement; (c) fundamental frequency; (d) volume fraction

Table 3: Summary of optimal design under volume, displacement and frequency constraints

Constraint	Compliance (Nmm)	Local displacement (mm)	Natural frequency (rad/s)
$\omega_1 > 1.6 \times 10^{-3}$ rad/s $d_A < 1.5\,mm$	149.57	1.4957	1.631×10^{-3}

5. CONCLUSION

This paper introduces the level set method handling multiple constraints such as displacement and frequency besides the common volume constraint in topology optimization of continuum structures. The Lagrange function is formed as a relaxed objective function that may contain any number of additional constraints. The Lagrange multipliers are determined by a search strategy using the sensitivities. In order to prevent searching in an infinite range, replacement factors within a finite range are suggested to show the Lagrange multipliers in the entire range through a scaling function. To evolve the topological design, an update scheme for element design variables and the additional Lagrange multipliers is applied through optimality criteria according to the relaxed objective function. Following the proposed general algorithms for level set method with multiple constraints, an optimization problem is constructed for minimization of compliance subject to additional constraints of local displacements and natural frequencies besides the common volume constraint. Therefore, element sensitivities of objective function and additional constraints are calculated. Lagrange multiplier update is determined following a search strategy based on the element sensitivities. To show the efficiency of proposed method, several numerical examples of 2D structures are examined for this type of multiple constraint optimization problem. Convergent solutions are obtained for compliance minimization that satisfies all the constraints. These examples clearly represent the effectiveness of the proposed method.

REFERENCES

1. Bendsøe MP, Kikuchi N. Generating optimal topologies in structural design using homogenization method, *Comp Meth Appl Mech Eng* 1988; **71**: 197-224.
2. Suzuki K, Kikuchi N. A homogenization method for shape and topology optimization, *Comp Meth Appl Mech Eng* 1991; **93**: 291-318.
3. Allaire G, Kohn RV. Optimal bounds on the effective behavior of a mixture of two well-ordered elastic materials, *Quat Appl Math* 1993; **51**: 643-674.
4. Allaire G, Bonnetier E, Francfort G, Jouve F. Shape optimization by the homogenization method, *Numer Math* 1997; **76**: 27-68.
5. Bendsøe MP, Kikuchi N. Generating optimal topology in structural design using a homogenization method, *Comp Meth Appl Mech Eng* 1988; **71**(2): 197-224.
6. Bendsøe MP, Sigmund O. Topology Optimization: *Theory, Methods, and Applications*, Springer, Berlin Heidelberg, 2003.
7. Xie YM, Steven GP. A simple evolutionary procedure for structural optimization, *Comput Struct* 1993; **49**(5): 885-96.
8. Kaveh A, Hassani B, Shojaee S, Tavakkoli SM. Structural topology optimization using ant colony methodology, *Eng Struct* 2008; **30**: 2559-65.
9. Yang XY, Xie YM, Steven GP, Querin OM. Bidirectional evolutionary method for stiffness optimization, *AIAA J* 1999; **37**: 1483–8.
10. Querin, OM, Young V, Steven GP, Xie YM. Computational efficiency and validation of bi-directional evolutionary structural optimization, *Comput Meth Appl Mech Eng* 2000; **189**: 559-73.
11. Huang X, Xie YM. Convergent and mesh-independent solutions for bi-directional evolutionary structural optimization method, *Finite Elements Anal Des* 2007; **43**(14): 1039-49.
12. Osher S, Fedkiw RP. *Level Set Methods and Dynamic Implicit Surface*, Springer-Verlag, New York, 2002.
13. Allaire G, Jouve F, Toader AM. Structural optimization using sensitivity analysis and a level-set method, *J Comput Phys* 2004; **194**: 363-93.
14. Wang MY, Wang XM, Guo DM. A level set method for structural topology optimization, *Comp Meth Appl Mech Eng* 2003; **192**: 217-24.
15. Shojaee S, Mohammadian M. A binary level set method for structural topology optimization, *Int J Optim Civil Eng* 2011; **1**(1): 73-90.
16. Shojaee S, Mohaghegh A, Haeri A. Piecewise constant level set method based finite element analysis for structural topology optimization using phase field method, *Int J Optim Civil Eng* 2015; **5**(4): 389-407.
17. Burger M, Hacker B, Ring W. Incorporating topological derivatives into level set methods, *J Comput Phys* 2004; **194**: 344-362.
18. Luo JZ, Luo Z, Chen LP, Tong LY, Wang MY. A semi-implicit level set method for structural shape and topology optimization, *J Comput Phys* 2008; **227**(11): 61-81.
19. Belytschko T, Xiao SP, Parimi C. Topology optimization with implicit function and regularization, *Int J Numer Meth Eng* 2003; **57**(8): 77-96.
20. Wang SY, Wang MY. Radial basis functions and level set method for structural topology optimization, *Int J Numer Meth Eng* 2006; **65**: 60-90.

21. Wang SY, Wang MY. Structural shape and topology optimization using an implicit free boundary parameterization method, *Comput Model Eng Sci* 2006; **13**: 19-47.
22. Luo Z, Wang MY, Wang SY, Wei P. A level set-based parameterization method for structural shape and topology optimization, *Int J Numer Meth Eng* 2008; **76**: 1-26.
23. Allaire G, de Gournay F, Jouve F, Toader AM. Structural optimization using topological and shape sensitivity via a level set method, *Control Cybern* 2005; **34**(1): 59-80.
24. Bendsøe MP, Sigmund O. Material interpolation schemes in topology optimization, *Archive Applied Mech* 1999; **69**: 635–654.
25. Luo JZ, Luo Z, Chen LP, Tong LY, Wang MY. A semi-implicit level set method for structural shape and topology optimization, *J Comput Phys* 2008; **227**(11): 61-81.
26. Luo Z, Tong L, Luo J, Wei P, Wang MY. Design of piezoelectric actuators using a multiphase level set method of piecewise constants, *J Comput Phys* 2009; **228**: 2643-26.
27. Huang X, Xie YM. Bi-directional evolutionary topology optimization of continuum structures with one or multiple materials*, Computat Mech* 2009; **43**: 393-401.
28. Huang X, Xie YM. Evolutionary topology optimization of continuum structures with an additional displacement constraint, *Struct Multidis Optim* 2010; **40**: 409-16.
29. Huang X, Zuo ZH, Xie YM. Evolutionary topological optimization of vibrating continuum structures for natural frequencies, *Comput Struct* 2010; **88**: 357-64.
30. Pedersen NL. Maximization of eigenvalues using topology optimization, *Struct Multidisc Optim* 2000; **20**: 2-11.
31. Yang XY, Xie YM, Steven GP, Querin OM. Topology optimization for frequencies using an evolutionary method, *J Struct Eng, ASCE* 1999; **125**: 1432-38.
32. Zuo ZH, Xie YM, Huang XD. An improved bidirectional evolutionary topology optimization method for frequencies, *Int J Struct Stability Dyn* 2010; **10**: 55-75.